

Three-Dimensional Numerical Simulation for Low Dopant Diffusion in Silicon

C. S. Yun, O. K. Kwon[†], C. G. Hwang, and H. J. Hwang[†]

Advanced Technology Center, Memory Division, Semiconductor Business,
Samsung Electronics Co., Ltd.
KyungKi, KOREA

[†]Department of Electronic Engineering, Chung Ang University
Seoul, KOREA

Abstract

A numerical simulator for the calculation of redistribution of low dopant diffusion in silicon has been developed in three-dimensional(3D) geometry. The diffusion behavior of boron is investigated by using three mask structures and changing the contact hole sizes. The results of calculations show that 3D diffusion effects will be very important in the development of submicron process and small device.

1. Introduction

Process simulation has already established itself as an indispensable tool for process and device development of VLSIs. With shrinking device dimensions, high dimensional simulations are required to predict the accurate profiles and the 3D effects[1], because it is very difficult for 2D simulations to predict the 3D effects or understand the 3D behaviors. And it is usually restricted by analytical 3D impurity profiles rather than actual profiles. This comes partly from the inexistence of effective numerical 3D process simulators. With this point of view we have developed 3D numerical simulator (VLSIDIF) for low dopant diffusion in silicon. In this paper, 3D mask structure effects of boron diffusion were investigated and hole size effects were simulated and discussed in comparison with 3D behavior of oxide growth.

2. Numerical Solution Method

The equation normally used to describe dopant diffusion is

$$\frac{\partial C}{\partial t} = \frac{\partial}{\partial x} \left(D \frac{\partial C}{\partial x} \right) + \frac{\partial}{\partial y} \left(D \frac{\partial C}{\partial y} \right) + \frac{\partial}{\partial z} \left(D \frac{\partial C}{\partial z} \right) \quad (1)$$

$$C(x,y,z) = C_o \quad : \quad \text{at the silicon surface} \quad (2)$$

$$C(x,y,z) = 0 \quad : \quad \text{at the silicon bulk} \quad (3)$$

$$\frac{\partial C}{\partial n} = 0 \quad : \quad \text{at the silicon sides and mask interfaces} \quad (4)$$

where C is the dopant concentration, D is the diffusion coefficient, and t is time. Diffusion equation is scaled with dimensionless scaling method to prevent the underflow or overflow[2]. In the numerical computation, the weighted residual formula of the Finite Element Method(FEM) is adopted to discretize the space domain and the finite difference method is applied to discretize the time domain in equation (1) [3]. It is assumed that normal flux to the boundary and mask interfaces are taken to be zero and the atoms arriving at the silicon surface is constant C_o Atoms/cm³. The final matrices formulation for diffusion equation (1) leads to

$$\left[\frac{1}{\Delta t_n} A_{ij} + K_{ij} \right] C_j^n = \left[\frac{1}{\Delta t_n} A_{ij} \right] C_j^{n-1} \quad (5)$$

where K_{ij} and A_{ij} are commonly known as the global stiffness and mass matrices and Δt is the time step. A fully implicit scheme is chosen in equation (5) as this can ensure an unconditionally stable and oscillation-free solution. A fast direct solver employing the frontal method is used to solve the global matrix and reduce the required core memory of computer[4]. This solver is particularly suited for solving the resultant matrix which is not only sparse but also banded. The FEM meshes based on automatic element subdivision of a few blocks were generated by 8 nodes rectangular parallelepiped elements.

3. Results and Discussion

Fig.1 shows 1D profile results of VLSIDIF compared with PROMIS1.5 and SUPREM-IV. The simulation was performed at 1000°C and 1100°C for 30 minutes and the surface concentration is maintained at $1e18$ Atoms/cm³. Fig.2 shows 2D simulated results of VLSIDIF compared with SUPREM-IV. In the case of VLSIDIF simulation, about 10,000 nodal points are used. The 1D & 2D simulated results of VLSIDIF show good agreement with those of other published 2D simulators. 3D diffusion behavior of low concentration dopant is investigated by using three mask structures which are called Hole, Island and Line Structure (HS, IS, LS). Fig.3 shows the three mask structure effects in the x-y planes along the silicon surface(z=0). In the LS, the 2D results of VLSIDIF are the same as normal 2D simulated results. But, In the IS, the dopants around the mask region are concentrated at the corner edge of mask region. And in the HS, the dopants from mask window are spreaded into the mask corner region. From these results it has been found that the diffusion at the corner of mask edge is much enhanced in the IS because of multiple supply of dopants and retarded in the HS because of lateral spread of dopants from the mask window. These three mask structure effects was similar to the oxidation mechanism of 3D mask structures[5]. Fig.3(d) shows 3D profiles of HS which well define the depth and lateral profiles. Fig.4 shows the 3D boron distribution as a function of the hole (contact) size. Fig.5 shows hole size vs. simulated junction depth and oxide thickness[5] which were normalized with each maximum data. As the hole size is narrower than about 1.0 μm, the junction depth of dopant is decreased and the shape of doping profiles along the silicon surface is getting to be rounded at the mask corner region. These 3D hole size effects were explained by restricted dopants from narrow mask window. With its 3D VLSIDIF simulations, we found out Impurity Dilute Phenomena (IDP)[6] and Impurity Circular Phenomena (ICP)

in narrow hole contact structures. These results suggest that IDP and ICP of narrow hole area should be considered in the design of bit line or direct contact structures for submicron devices. In fig.6 elapsed time for simulation of the 3D diffusion process are demonstrated as a total grid number on SUN/IPC system. Elapsed time are drastically increased above the 5000 nodal points. To reduce the CPU time, more efficient matrix solver is required for 3D process simulation.

4. conclusion

The 3D diffusion simulator, VLSIDIF, has been developed to predict small -size process/device characteristics. The mask structure effect and the small contact hole size effect on the device fabrication have been found by varying simulation conditions. In addition, We know that the 3D diffusion phenomena was similar to the 3D effect on the oxide growth. ICP and IDP have been also found as a hole contact size and we know that they are very important in the small geometry processes.

Reference

- [1] M.R. Pinto, J. Bude and C.S. Rafferty,"Simulation of ULSI Silicon MOSFET's," VPAD, pp22-25, May, 1993.
- [2] J. Crank, The Mathematics of Diffusion, Oxford University Press, London, pp138-152, 1976.
- [3] R. Ismail and G. Amaratunga," Adaptive Meshing Schemes for Simulating Dopant Diffusion," IEEE Trans. on CAD, Vol. 9, No. 3, pp276-289, March, 1990
- [4] C. Taylor and T.G. Hughes,"Finite Element Programming of the Navier-Stokes Equations," Printed in Great Britain, pp120-153, 1981.
- [5] H. Umimoto and S. Odanaka," Three-Dimensional Numerical Simulation of Local Oxidation of Silicon," IEEE Trans. on Elec. Devices, Vol. 38, No. 3, pp505-511, March, 1991.
- [6] S. Onga and Taniguchi,"A Three-Dimensional Process Simulator and Its Application to Submicron VLSI's," in Digest Tech. papers Symposium on VLSI Technology, pp68-69, 1985.

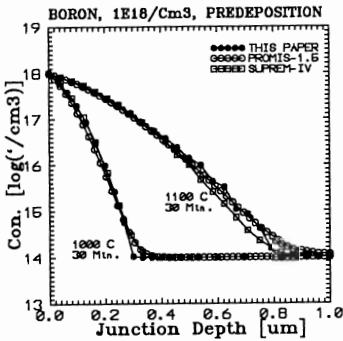


Fig.1 1-dimensional simulated profiles of VLSIDIF(●), PROMIS1.5(O) and SUPREM-IV(□).

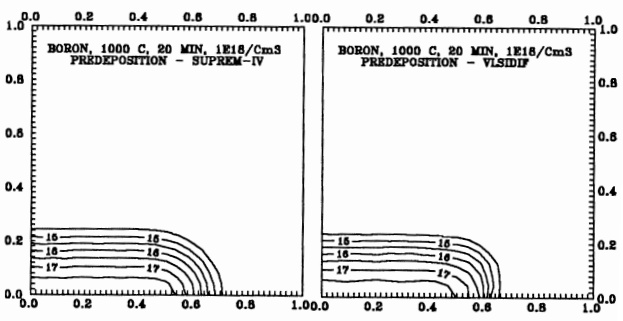


Fig.2 Comparison of 2D simulated results of VLSIDIF with SPREM-IV after boron predeposition.

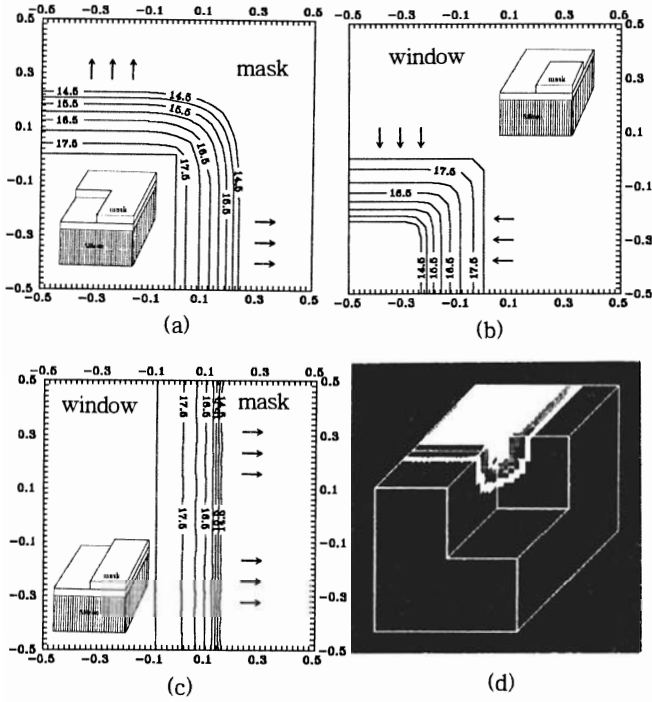
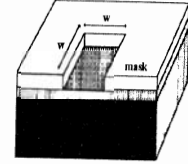
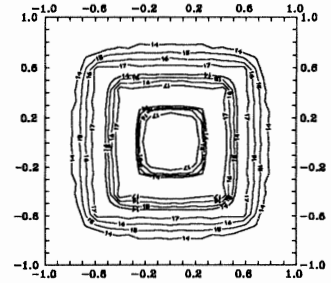


Fig.3 Simulation results of 3D distribution after boron predeposited 1000 °C for 30 minutes on the three different mask structures.



(a)



(b)

Fig.4 Simulated results of hole size effects on the silicon surface (hole size : 1.0x1.0 μm , 0.7x0.7 μm , 0.3x0.3 μm was overlapped).

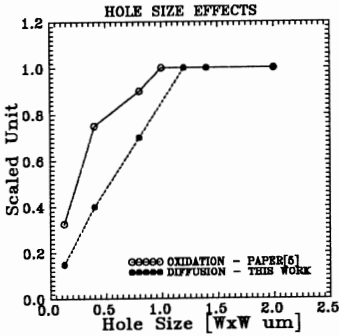


Fig.5 Hole contact size ($W \times W$) vs. junction depth and oxide thickness [5].

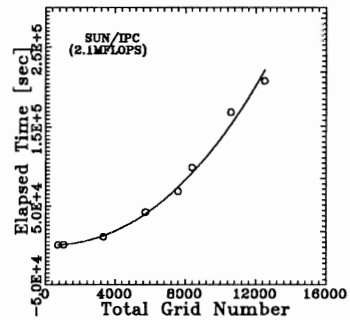


Fig.6 Evaluated CPU time with varying the number of total nodal points.